energies

MDPI

*Article*

# Effect of Mainstream Velocity on the Heat Transfer Coefficient of Gas Turbine Blade Tips

**Jin Young Jeong [1], Woojun Kim [1], Jae Su Kwak [1,*], Byung Ju Lee [2] and Jin Taek Chung [2]**

[1] School of Aerospace and Mechanical Engineering, Korea Aerospace University, Goyang 10540, Korea; jyjeong1220@kau.kr (J.Y.J.); universe1217@kau.kr (W.K.)
[2] Department of Mechanical Engineering, Korea University, Seoul 02841, Korea; jdbjlee11@korea.ac.kr (B.J.L.); jchung@korea.ac.kr (J.T.C.)
* Correspondence: jskwak@kau.ac.kr

**Abstract:** This study experimentally investigated the effects of cascade inlet velocity on the distribution and the level of the heat transfer coefficient on a gas turbine blade tip. The tests were conducted in a transient turbine test facility at Korea Aerospace University, and three cascade inlet velocities—30, 60, and 90 m/s—were considered. The heat transfer coefficient was measured using the transient IR camera technique with a linear regression method, and both the squealer and plane tips were investigated. The results showed that the overall averaged heat transfer coefficient was generally proportional to the inlet velocity. As the inlet velocity is increased from 30 m/s to 60 m/s and 90 m/s, the heat transfer coefficient increased by 11.4% and 25.0% for plane tip, and 26.6% and 64.1% for squealer tip, respectively. However, the heat transfer coefficient near the leading edge of the squealer tip and the reattachment region of the plane tip was greatly affected by the cascade inlet velocity. Therefore, heat transfer experiments for a gas turbine blade tip should be performed under engine simulating conditions.

**Keywords:** gas turbine; heat transfer; blade tip; high speed condition



**Citation:** Jeong, J.Y.; Kim, W.; Kwak, J.S.; Lee, B.J.; Chung, J.T. Effect of Mainstream Velocity on the Heat Transfer Coefficient of Gas Turbine Blade Tips. *Energies* **2021**, *14*, 7968. https://doi.org/10.3390/en14237968

Academic Editor: Andrea De Pascale

Received: 18 October 2021
Accepted: 19 November 2021
Published: 29 November 2021



## 1. Introduction

The tip leakage flow (TLF) through the gap between the rotating blade tip and stationary turbine casing induces a high and uneven heat transfer coefficient (HTC) on the tip surface and results in high thermal stress on the blade tip surface. Since the TLF is driven by pressure differences between the pressure side (PS) and suction side (SS), as well as between the leading edge and trailing edge, it is mainly affected by the profile of the turbine blade tip and flow conditions near the tip region.

It is widely known that blade tip loss has a significant effect on gas turbine efficiency. Occasionally, the rubbing between a blade tip and the stationary casing is permitted to minimize the gap and improve the efficiency of the turbine [1]. Therefore, a blade tip should be designed to be robust so as not to be damaged by the friction and oxidation caused by extremely high temperature operating conditions [2].

Many studies on various blade tip shapes and geometrical factors have been conducted to garner a fundamental understanding of the TLF. Bunker et al. [3] measured the HTC of the plane tip and observed a low HTC region near the leading edge. Kwak et al. [4,5] measured the HTC of various squealer tips with GE-$E^3$ blade profiles and determined that all considered tips showed increased HTC values near the tip region as the tip clearance increased. They also presented the effects of squealer rim locations and height on the tip HTC and analyzed flow patterns based on heat transfer results. Ameri et al. [6] performed a numerical study for a blade tip with a recessed casing by solving a Reynolds-Averaged Navier–Stokes (RANS) equation. The introduction of the casing recess resulted in the reduction of the PS heat transfer, but more complex flow patterns were generated at the shroud. Key and Arts [7] performed an oil-dots flow visualization and static pressure

measurements at the tip region to understand the complex vortex patterns of the plane tip and squealer tip. They also compared the pressure distributions of the squealer tip and plane tip in two levels of inlet Reynolds numbers.

Many researchers have also suggested new tip shapes to improve tip cooling and aerodynamic performance. Park et al. [8] proposed a multi-cavity tip with ribs in the cavities. The ribs enhanced the flow resistance of the cavities, and it was confirmed that a multi-cavity tip could reduce both aerodynamic losses and the HTC compared to a squealer tip. Saha et al. [9] conducted a numerical study to investigate the effect of a PS winglet on the tip heat transfer. They showed that the winglet had reduced the averaged HTC and the pressure ratio by 7% and 10%, respectively. Yan et al. [10] also investigated the effects of the coolant ejection angle and blowing ratio on the heat transfer and film cooling effects for a winglet tip. They showed that high film cooling effectiveness with a low heat transfer coefficient was observed at the streamwise ejection angle of 120°. Prakash et al. [11] suggested an improved blade tip model with an inclined shelf on the PS. They tested both straight and inclined shelf tips, and only the inclined shelf model exhibited a reduced tip leakage flow, which was due to the generation of a large vortex along the PS rim. Jeong et al. [12] proposed a partial cavity tip that combined the advantages of a plane tip and a squealer tip. They experimentally showed that the partial cavity tip could reduce the HTC by 15% compared with the squealer tip.

Studies on the flow characteristics under engine operating conditions have also been conducted. Zhang et al. [13] numerically and experimentally studied the structures of shock waves between the plane tip and shroud. It was shown that the tip heat transfer upstream from the shock was reduced via the flow acceleration, but the adverse pressure gradient restored by the shock wave induced a high HTC region. Zeng et al. [14] performed a flow visualization inside the squealer tip gap using particle image velocimetry to observe the effects of relative motion between the blade tip and shroud. They demonstrated that the reattachment and recirculation of leakage flow moved toward the PS direction due to the relative motion of the shroud. Rhee and Cho [15] measured time-averaged heat and mass transfer coefficients using a naphthalene sublimation technique in a low-speed rotating turbine blade cascade, and they compared the results with those of stationary blades. They showed that the HTC on the blade tip was 1.7 times higher than the HTC values for the blade surface and the shroud. In addition, due to the relative motion of the shroud, the tip HTC of the rotating cascade was 10% lower than that of the stationary cascade.

By using the recently advanced computational fluid dynamics (CFD) technique, numerical studies on heat transfer of turbine components are being widely conducted [16,17]. Experimental approaches are still required to verify the CFD results, but many of them are still being performed under low-speed conditions due to the limitations in measurement devices and test facilities.

In the present study, experiments were conducted to measure the HTCs of the plane tip and the squealer tip under different inlet velocity conditions. Based on the measured results, detailed heat transfer and flow pattern changes according to the different inlet mainstream velocities were analyzed.

## 2. Experimental Setup and Heat Transfer Measurement Technique

### *2.1. High Speed Blow-Down Cascade Facility*

Figure 1 presents the schematics of the transonic turbine cascade test rig used to measure the blade tip heat transfer. Before the test, the air from the compressors (30 HP, 2EA) is supplied to the air receiver tanks (60 $m^3$) up to a pressure of 9.5 bar in absolute pressure. Compressed air is then supplied to the cascade after passing through a flow rate control valve and an air heater. The opening of the control valve is managed automatically via a LabVIEW-based control system that receives feedback from the mainstream velocity in the test section. A safety valve is additionally installed for the air supply section. If the pressure in the air supply section exceeds the present value, the safety valve is activated, and the compressed air bypasses the air supply section to protect the test section.

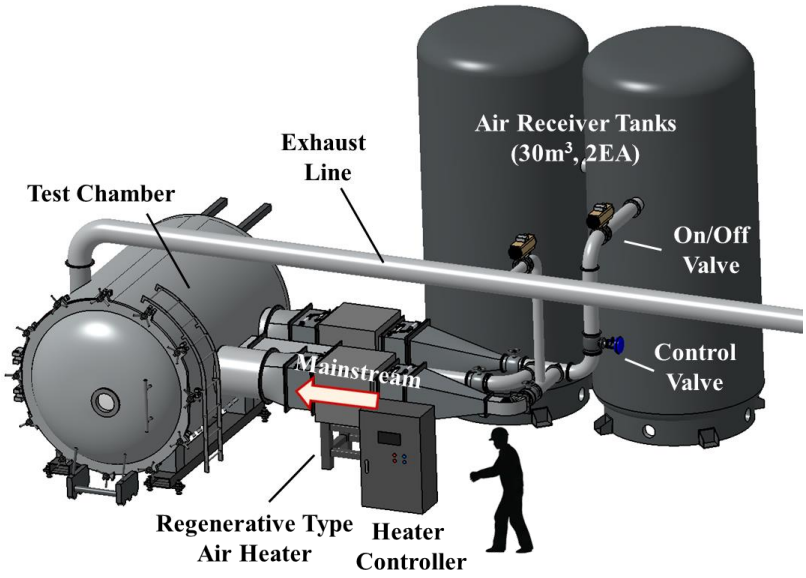


(**a**)

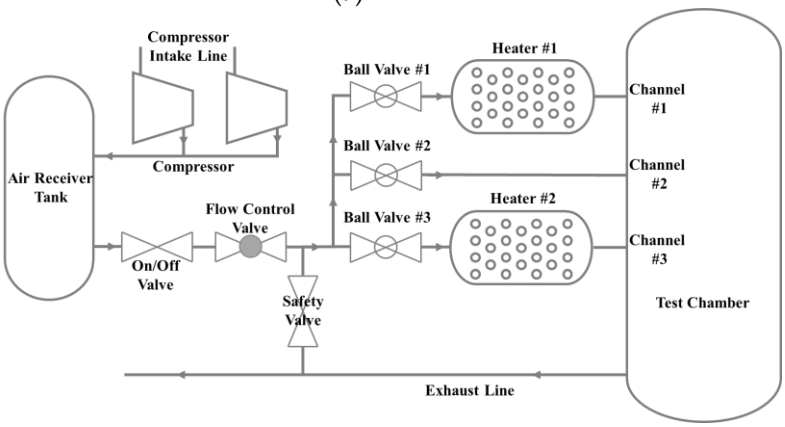


(**b**)

(**c**)

**Figure 1.** Schematic of test facility (**a**) Layout of test facility; (**b**) Schematic diagram of test facility; (**c**) Actual picture of test rig.

The test section has three channels (Figure 1b). The first and third test channels have regenerative-type heaters for heat transfer experiments. In this study, the final mainstream temperature of each velocity condition was maintained at about 70 °C by adjusting the heater rod temperature.

Three mainstream velocity condition levels—30, 60, and 90 m/s—were considered. Figure 2 shows the mainstream velocity at the cascade inlet, the pressure of the air tank, and the mainstream temperature at the cascade inlet during each test condition. The mainstream velocity reached the target value within two seconds after the on/off valve opened. During the transient test, the pressure of the air tank continuously decreased, but the mainstream velocity was kept constant by adjusting the opening of the control valve.

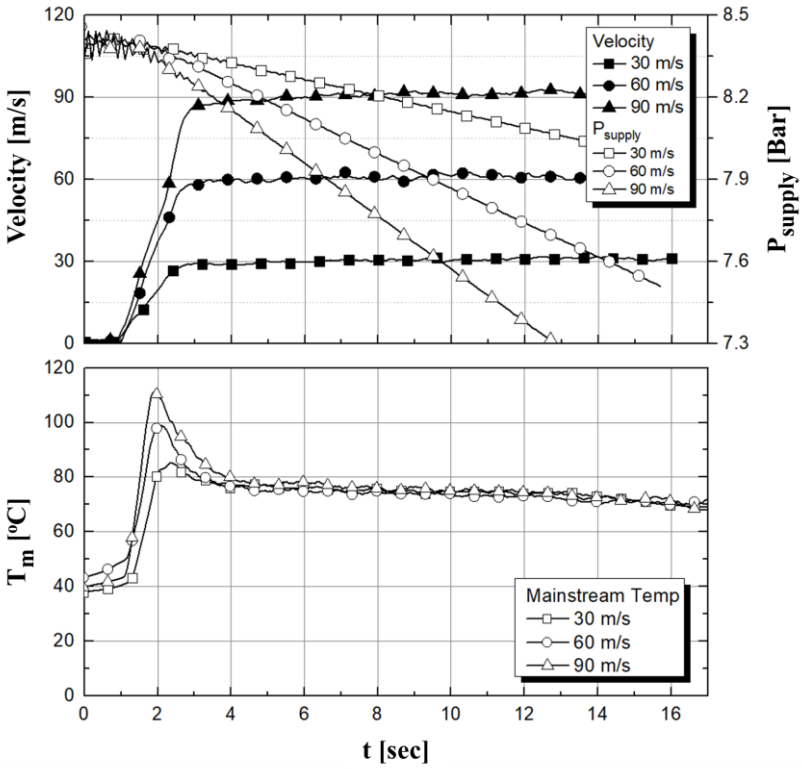


**Figure 2.** Mainstream velocity and temperature history during the test.

Figure 3 represents the schematic diagram of the test section. The heated air was supplied to the cascade after passing the inlet duct with a bell-mouth and a turbulence grid (Figure 3a). The cascade consisted of six blades with a GE-E$^3$ high pressure turbine (HPT) blade profile [16]. Equation (1) was used to calculate the mainstream velocity. The dynamic and static pressure was measured using a pitot-tube (PAC-8-KL, United Sensor) and pressure gauges (PX-309/PX409, OMEGA).

$$V_{in} = \sqrt{\frac{2(P_t - P_s)R\,T_m}{P_s}} \quad (1)$$

The tested cascade had five passages, and the tip clearance was 2 mm (1.25% of span). The blades were designed for the tip portion to be replaceable. The support blade was made of aluminum, and the replaceable component was made of acrylic, which is advantageous for heat transfer experiments due to the low conductivity (Figure 3b). The thermal conductivity (k), thermal diffusivity, and density of the test blade were 0.196 W/m·K, $0.126 \times 10^{-6}$ m$^2$/s, and 1180 kg/m$^3$, respectively.

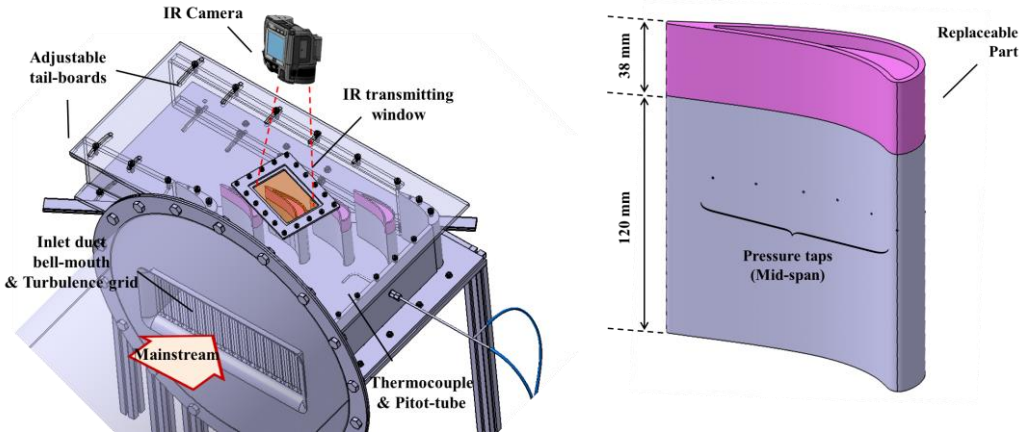


**Figure 3.** Schematic of test section (**a**) Experimental test setup; (**b**) Heat transfer measurement blade.

The tip shapes tested in this study were plane and squealer, which are commonly used in aero- and land-based gas turbines. The tips of the adjacent blades were also replaced to ensure the same tip shape as the test blade. To compare the HTC between the engine simulating Mach number condition [18] (90 m/s) and low-speed conditions, two lower inlet velocity levels of 30 and 60 m/s were selected. Detailed specifications of the cascade and flow conditions are shown in Table 1.

**Table 1.** Specifications of cascade and flow conditions.

| | |
|---|---|
| Blade chord | 126 (mm) |
| Blade span | 160 (mm) |
| Blade pitch | 102.7 (mm) |
| Number of blades | 6 |
| Cascade inlet angle | 32° |
| Cascade exit angle | 97.7° |
| Tip clearance | 1.25 (% of span) |
| Inlet velocity ($V_{in}$) | 30/60/90 (m/s) |
| Inlet Reynolds number ($Re_c$) | 1.82/3.80/5.93 ($\times 10^5$) |
| Inlet Mach number (Ma) | 0.08/0.16/0.25 |

A zinc-selenide infra-red transmitting window was placed in the casing over the tip to facilitate the IR camera measurements, and the variation in the tip surface temperature was measured using an IR camera (T650sc, FLIR). The turbulence intensity measured with a hot-wire velocimeter (StreamLine Pro, Dantec) was 11.1% at the mainstream velocity condition of 90 m/s.

A thermocouple for the in situ calibration [19] of IR-measured temperatures was attached to the trailing edge of the blade tip. Figure 4 presents the relationship between the temperatures measured by IR camera and the thermocouple attached on the trailing edge of blade tip.

Before the heat transfer test, the flow condition of the cascade was confirmed by comparing the experimentally measured pressure coefficient (Equation (2)) along the mid-span of the blade with results from the CFD with the periodic condition. Cascade tailboards were adjusted to match the pressure coefficient distribution of the CFD results. Figure 5 shows the distribution of the pressure coefficient on the blade mid-span calculated using the commercial CFD code, ANSYS CFX 2019 R1.

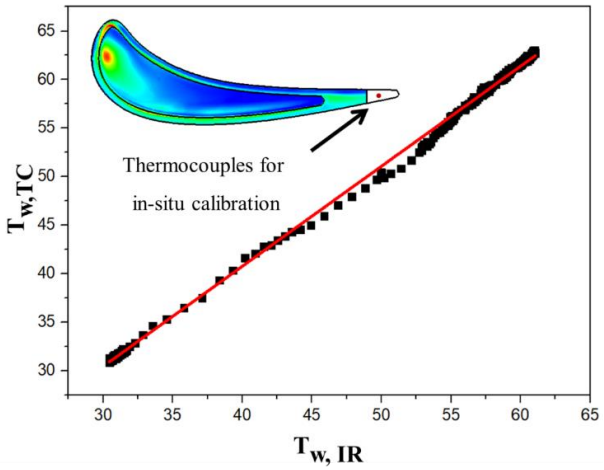


**Figure 4.** In situ calibration of IR camera and thermocouples.

$$c_p = \frac{P_w - P_t}{P_t - P_s} \tag{2}$$

*2.2. HTC Measurement*

To calculate the HTC, many researchers use the linearity between the heat flux (q″) and the difference between the adiabatic wall temperature and wall temperature ($T_{adw} - T_w$), as shown in Equation (3) [19–21]. From Equation (3), the heat flux (q″) and temperature difference between the mainstream and wall ($T_m - T_w$) can be expressed in a linear relation, as shown in Equation (4).

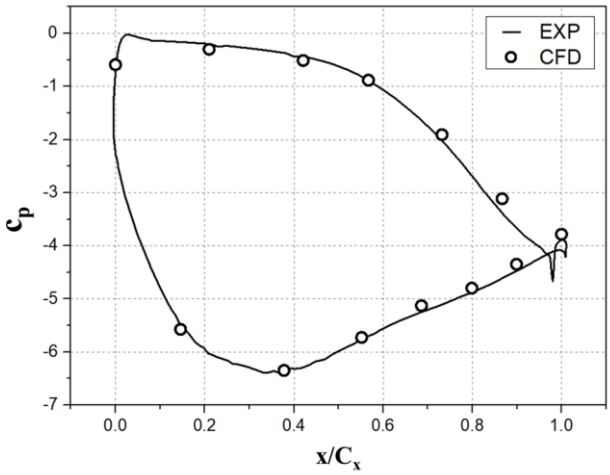


**Figure 5.** Pressure coefficient via CFD and experiment.

In this study, the wall temperature was measured using an IR camera with a frequency of 30 Hz, and the heat flux was numerically calculated via the 1D-finite volume method (Equations (5) and (6)) from the measured wall temperature at each time step.

Finally, the temperature difference ($T_m - T_w$) and heat flux (q″) pairing at each time step could be plotted as shown in Figure 6, and the HTC was the slope of the line obtained from the linear regression of the data.

$$q'' = h(T_{adw} - T_w) \tag{3}$$

$$q'' = h(T_m - T_w) - h(T_m - T_{adw}) \tag{4}$$

$$\rho c_p \frac{\partial T}{\partial t} = k \frac{\partial^2 T}{\partial z^2} \tag{5}$$

$$\begin{cases} T(t,0) = T_w \\ T(t,\infty) = T_i \\ T(0,z) = T_i \end{cases} \quad (6)$$

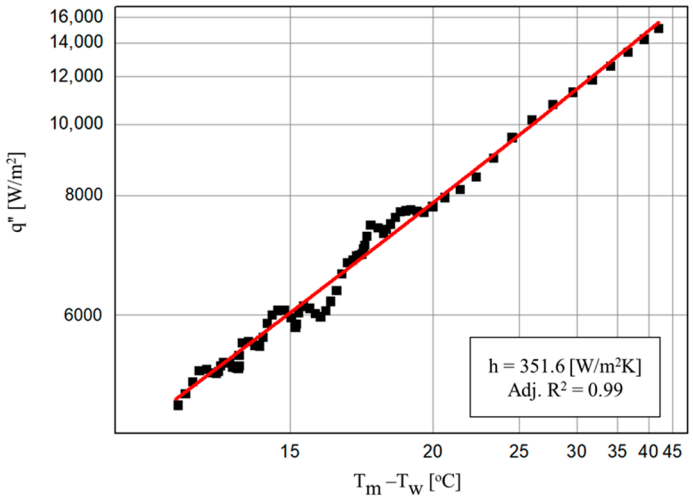


**Figure 6.** Linearity of the heat flux ($q''$) and temperature difference ($T_m - T_w$).

The uncertainty of the measured heat transfer coefficient was estimated using Equations (7) and (8) [21–23]. To estimate the uncertainty, measurement uncertainties $\Delta T_m$, $\Delta M$, $\Delta t$, and $\Delta T_w$ were assumed to be 0.3 °C, 5%, 1/30 s, and 0.5 °C, respectively. The resulting uncertainties were 13.4% and 8.97% for the HTC at 1192 W/m$^2$K and 279 W/m$^2$K, respectively.

$$\Delta h = \sqrt{\left(\frac{\partial h}{\partial T_w}\Delta T_w\right)^2 + \left(\frac{\partial h}{\partial M}\Delta M\right)^2 + \left(\frac{\partial h}{\partial t}\Delta t\right)^2 + \left(\frac{\partial h}{\partial T_m}\Delta T_m\right)^2} \quad (7)$$

$$\frac{\partial h}{\partial T_w} = \sqrt{\left(\frac{\partial h}{\partial T_{w,1}}\Delta T_{w,1}\right)^2 + \left(\frac{\partial h}{\partial T_{w,2}}\Delta T_{w,2}\right)^2 + \ldots + \left(\frac{\partial h}{\partial T_{w,n}}\Delta T_{w,n}\right)^2} \quad (8)$$

## 3. Results and Discussion

### *3.1. Plane Tip*

Figure 7 shows the HTC contours measured by the linear regression method at three different $V_{in}$ conditions. The plane tip had a low HTC region near the leading edge and a high HTC along the PS. These results have been reported in many previous studies. The HTC of the plane tip showed simple and predictable increases with the increases in $V_{in}$. As shown in Figure 8, as the $V_{in}$ increased, the HTC of the plane tip generally increased, and the increase in the HTC downstream from the reattachment region was particularly noticeable. Figure 9a,b show the HTC along the $x/C_x = 0.25$ and $x/C_x = 0.5$ lines, respectively. Low HTC regions were observed along the PS ($0 < y/P < 0.02$), which were caused by the separation of the TLF. It seemed that the effect of $V_{in}$ on the size of the separation bubble was insignificant, and the maximum HTC was observed at a similar $y/P$ location. The HTC near the reattachment region for the $V_{in}$ = 90 m/s case showed a much larger value than it did for the other two cases. This was possibly due to the stronger vortex structure within the tip clearance.

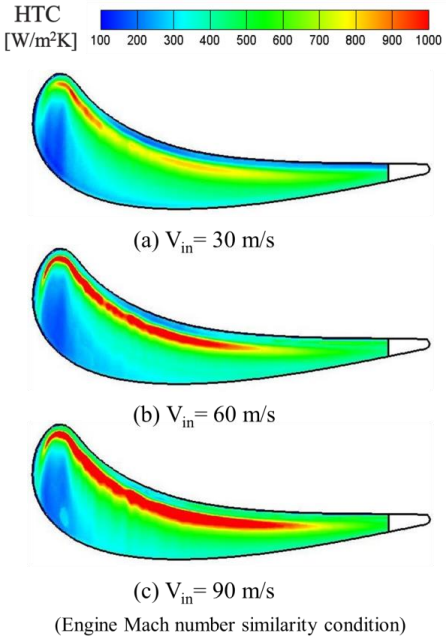


**Figure 7.** HTC contours of the plane tip.

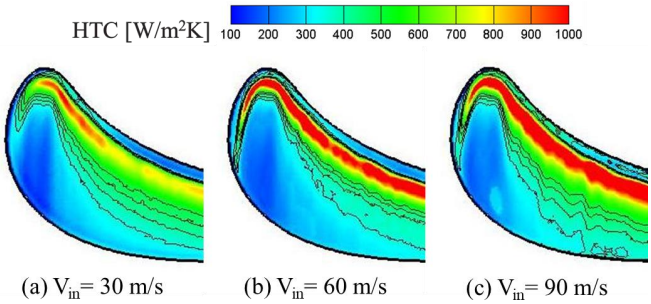


**Figure 8.** Detailed HTC of the plane tip at each velocity condition ($x/C_x < 0.4$, plane tip).

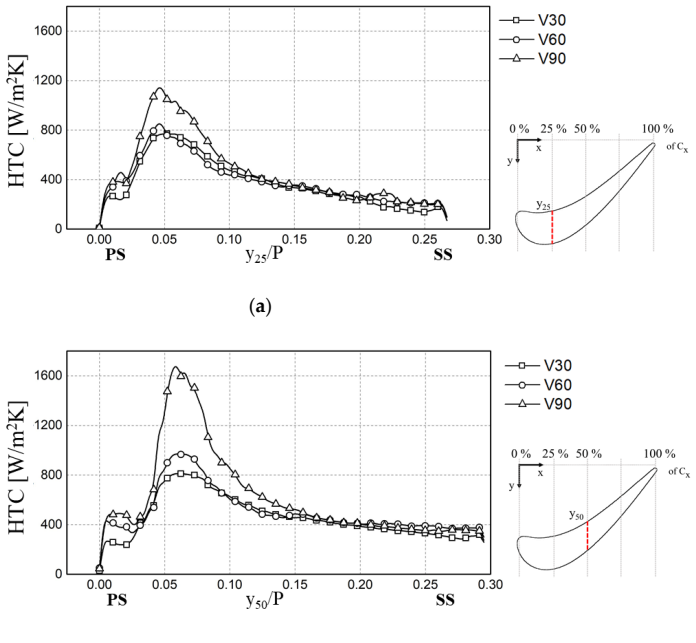


**Figure 9.** HTC of the plane tip in the y-direction (**a**) 25%of $C_x$; (**b**) 50% of $C_x$.

### *3.2. Squealer Tip*

Figure 10 shows the HTC contours of the squealer tip at each inlet velocity condition. At the squealer tip, a high HTC in frontal region was observed due to the TLF reattachment at the cavity surface. After the mid-chord region, the HTC of the cavity surface increased monotonically as the inlet velocity increased.

Researchers have observed three different vortices in squealer tips for various blade tip shapes, which have been named the leading edge vortex (LEV), cavity vortex (CV), and cavity scraping vortex (CSV) [24].

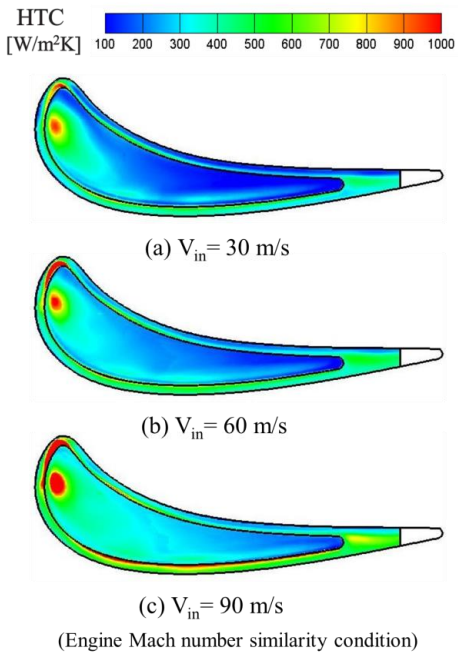


**Figure 10.** HTC contours of squealer tip.

Figure 11 shows the detailed HTC distribution over the frontal region of the squealer tip. In Figure 11, the red dashed lines represent the estimated paths of each vortex. In the case of $V_{in}$ = 60 m/s (Figure 11b), the traces of the three vortices (LEV, CV, and CSV) explained by Zhong and Zhou [24] were observed. As the TLF separated and reattached to the tip surface, the LEV and the CSV appeared along the suction side rim and camber line, respectively. Also, the CV formed along the PS squealer rim. Those vortices were strongly affected by the leakage condition, i.e., the inlet mainstream velocity, and they were related to one another in a complex manner. Consequently, the HTC on the tip was also affected by those vortices and the inlet mainstream velocity condition. In the case of $V_{in}$ = 30 m/s or $V_{in}$ = 90 m/s, only some of those vortices were observed due to the different vortex structure.

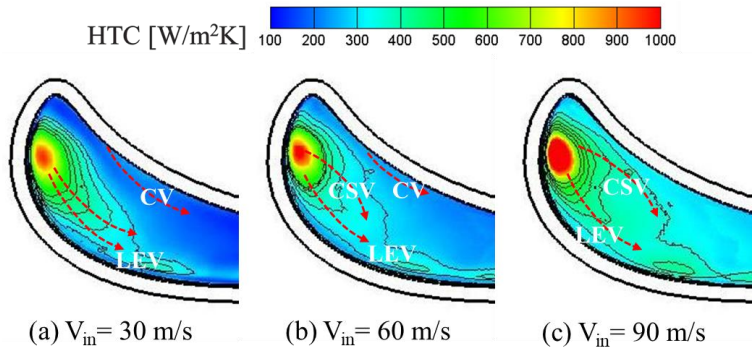


**Figure 11.** Detailed HTC of squealer tip at each velocity condition (x/Cx < 0.4, squealer tip).

The most significant change in the vortex structure due to the increase in $V_{in}$ was the strengthening of the CSV. Figure 12 shows the HTC along the y-direction of the squealer tip at the frontal region ($x/C_x = 0.25$, Figure 12a) and mid-chord region ($x/C_x = 0.5$, Figure 12b). In the case of $V_{in}$ = 60 m/s, the HTC near the SS in the frontal region was smaller than that of the 30 m/s case (Figure 12a). At the frontal region, it seemed that the stronger LEV pushed the CSV away from the tip surface in the case of $V_{in}$ = 30 m/s, and that caused a different HTC distribution for the case. Unlike the frontal region, the HTC after the mid-chord region increased as the $V_{in}$ increased.

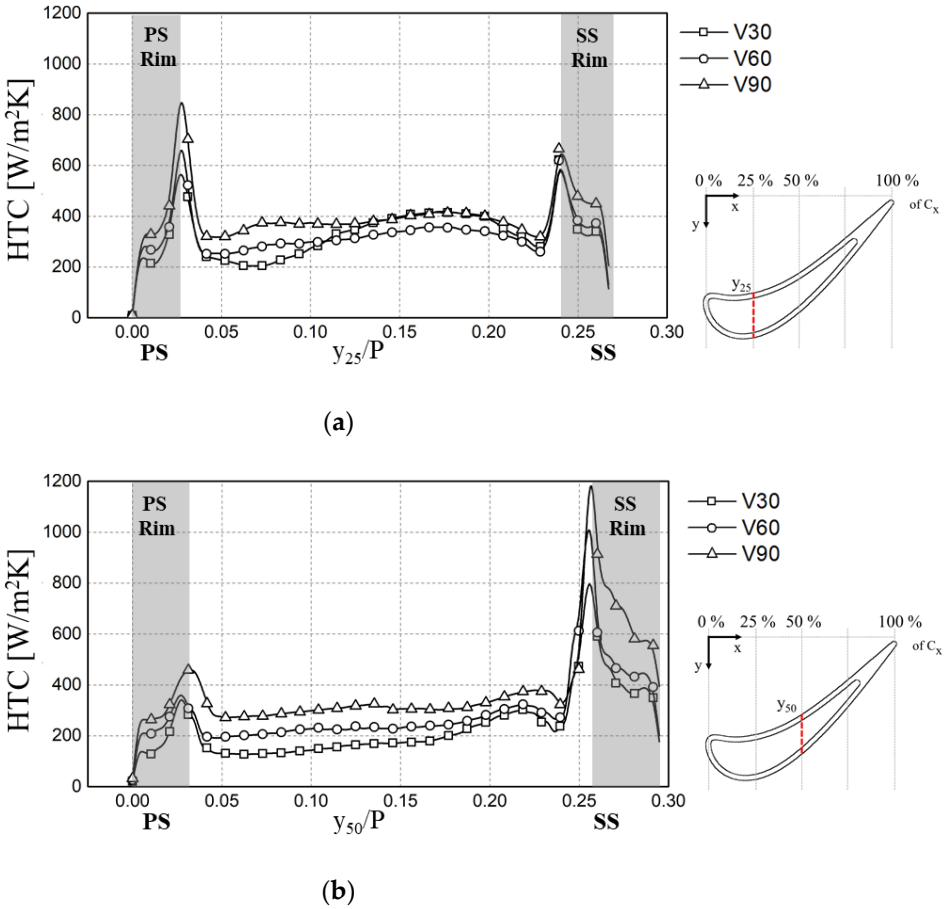


**Figure 12.** HTC of the squealer tip in the y-direction (**a**) 25%of $C_x$; (**b**) 50% of $C_x$.

As explained above, the size and strength of the vortices were related in a complicated manner, and they were strongly affected by the level of inlet mainstream velocity. Therefore, the HTC at the frontal region (Figure 12a) where the vortex structure was more complex was more likely affected by the inlet mainstream velocity.

### *3.3. Overall Averaged HTC*

Figure 13 shows the averaged HTC values of both blade tips. In Figure 13, the upper triangle symbol indicates the overall averaged HTC of the frontal region ($x/C_x < 0.5$), and the lower triangle symbol indicates that of the rear region ($x/C_x > 0.5$). The HTC of the rear region showed roughly liner increases as $V_{in}$ increased, but the increase in the HTC in the frontal region greatly increased due to the change of vortex structures. Therefore, the overall averaged HTC for $V_{in}$ = 90m/s was much higher than in the other cases.

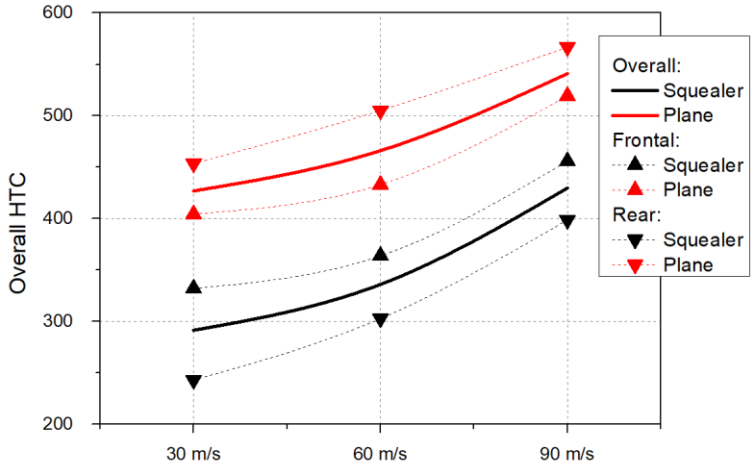


**Figure 13.** Overall averaged HTC of blade tips.

## 4. Summary

In this study, the HTC distributions of the squealer tip and plane tip were measured under three different inlet mainstream velocity conditions—30, 60, and 90 m/s. The tested linear cascade had a GE-E$^3$ HPT blade tip profile, and the HTC contours of the blade tip were measured using the heat flux linear regression method. Based on the measured results, the following conclusions were obtained.

1. For the squealer tip, the vortex structure in the frontal region of the tip was significantly affected by the inlet mainstream velocity, and, as a result, the heat transfer coefficient in the region was also greatly altered by the cascade inlet condition.
2. For the plane tip, the size of the vortex near the blade mid-chord increased as the inlet mainstream velocity increased, resulting in a significant increase in heat transfer.
3. The overall averaged HTC tended to be proportional to the inlet mainstream velocity, but the local HTC, particularly in the frontal region, was greatly affected by the inlet mainstream velocity. Therefore, experimental studies should be conducted under engine simulating conditions.

**Author Contributions:** Conceptualization, J.Y.J., J.S.K. and J.T.C.; methodology, J.Y.J. and W.K.; software, J.Y.J. and B.J.L.; validation, J.Y.J., W.K. and B.J.L.; formal analysis, J.Y.J. and J.S.K.; investigation, J.Y.J. and W.K.; resources, J.S.K. and J.T.C.; data curation, J.Y.J. and W.K.; writing—original draft preparation, J.Y.J. and J.S.K.; writing—review and editing, J.Y.J. and J.S.K.; visualization, J.Y.J.; supervision, J.S.K.; project administration, J.S.K. and J.T.C.; funding acquisition, J.S.K. and J.T.C. All authors have read and agreed to the published version of the manuscript.

**Funding:** This work has been supported by the UAV High Efficiency Turbine Research Center program of the Defense Acquisition Program Administration and Agency for Defense Development.

**Institutional Review Board Statement:** Not applicable.

**Informed Consent Statement:** Not applicable.

**Data Availability Statement:** Not applicable.

**Conflicts of Interest:** The authors declare no conflict of interest.

## Nomenclature

| | |
|---|---|
| CSV | Cavity scraping vortex |
| CV | Cavity vortex |
| HTC | Heat transfer coefficient |
| LEV | Leading edge vortex |
| PS | Pressure side |
| SS | Suction side |
| TLF | Tip leakage flow |

**Symbols**

| | |
|---|---|
| C | Blade chord |
| $c_p$ | Specific heat of test plate, J/g·K |
| h | Heat transfer coefficient, $W/m^2K$ |
| k | Thermal conductivity of test plate, W/m·K |
| M | Thermal properties of solid, $\sqrt{\alpha}/k$ |
| P | Pressure, Pa |
| q" | Heat flux, $W/m^2$ |
| R | Gas constant, J/g·K |
| t | Test time, sec |
| T | Temperature, °C |
| V | Velocity, m/s |
| x | Location in axial direction, mm |
| y | Location in pitch direction, mm |
| z | Location in span direction, mm |

**Greeks**

| | |
|---|---|
| $\alpha$ | Thermal diffusivity of test plate, $m^2/s$ |

**Subscripts**

| | |
|---|---|
| adw | Adiabatic wall |
| i | Initial condition |
| in | Inlet |
| m | Mainstream |
| s | Static properties |
| t | Total properties |
| w | Wall |

## References


1. Bunker, R.S. Axial Turbine Blade Tips: Function, Design, and Durability. *J. Propuls. Power* **2006**, *22*, 271–285. [CrossRef]
2. Bunker, R.S.; Bailey, J.C. Effect of Squealer Cavity Depth and Oxidation on Turbine Blade Tip Heat Transfer. In *Volume 3: Heat Transfer; Electric Power; Industrial and Cogeneration, Proceedings of the ASME Turbo Expo 2001: Power for Land, Sea, and Air, New Orleans, LA, USA, 4–7 June 2021*; American Society of Mechanical Engineers: New York, NY, USA, 2001; p. V003T01A038.
3. Bunker, R.S.; Bailey, J.C.; Ameri, A.A. Heat Transfer and Flow on the First-Stage Blade Tip of a Power Generation Gas Turbine: Part 1—Experimental Results. *J. Turbomach.* **2000**, *122*, 263–271. [CrossRef]
4. Kwak, J.S.; Ahn, J.; Han, J.-C. Effects of Rim Location, Rim Height, and Tip Clearance on the Tip and near Tip Region Heat Transfer of a Gas Turbine Blade. *Int. J. Heat Mass Transf.* **2004**, *47*, 5651–5663. [CrossRef]
5. Kwak, J.S.; Ahn, J.; Han, J.-C.; Lee, C.P.; Bunker, R.S.; Boyle, R.; Gaugler, R. Heat Transfer Coefficients on the Squealer Tip and Near-Tip Regions of a Gas Turbine Blade With Single or Double Squealer. *J. Turbomach.* **2003**, *125*, 778–787. [CrossRef]
6. Ameri, A.A.; Steinthorsson, E.; Rigby, D.L. Effects of Tip Clearance and Casing Recess on Heat Transfer and Stage Efficiency in Axial Turbines. In *Volume 4: Heat Transfer; Electric Power; Industrial and Cogeneration, Proceedings of the ASME 1998 International Gas Turbine and Aeroengine Congress and Exhibition, GT 1998, Stockholm, Sweden, 2–5 June 1998*; American Society of Mechanical Engineers: New York, NY, USA, 1998; p. V004T09A066.
7. Key, N.L.; Arts, T. Comparison of Turbine Tip Leakage Flow for Flat Tip and Squealer Tip Geometries at High-Speed Conditions. *J. Turbomach.* **2006**, *128*, 213–220. [CrossRef]
8. Park, J.S.; Lee, S.H.; Kwak, J.S.; Lee, W.S.; Chung, J.T. Measurement of Blade Tip Heat Transfer and Leakage Flow in a Turbine Cascade With a Multi-Cavity Squealer Tip. In Proceedings of the ASME 2013 Turbine Blade Tip Symposium, Hamburg, Germany, 30 September–3 October 2013; p. V001T02A006.
9. Saha, A.K.; Acharya, S.; Bunker, R.; Prakash, C. Blade Tip Leakage Flow and Heat Transfer with Pressure-Side Winglet. *Int. J. Rotating Mach.* **2006**, *2006*, 017079. [CrossRef]
10. Yan, X.; Huang, Y.; He, K. Effect of Ejection Angle and Blowing Ratio on Heat Transfer and Film Cooling Effect on a Winglet Tip. *Int. J. Heat Mass Transf.* **2018**, *125*, 357–374. [CrossRef]
11. Prakash, C.; Lee, C.-P.; Cherry, D.; Wadia, A.; Doughty, R. Analysis of Some Improved Blade Tip Concepts. In *Volume 6: Turbo Expo 2005, Parts A and B, Proceedings of the ASME Turbo Expo 2005: Power for Land, Sea, and Air, Reno, NV, USA, 6–9 June 2005*; ASMEDC: Chevy Chase, MD, USA, 2005; pp. 529–533.
12. Jeong, J.Y.; Kim, W.; Kwak, J.S.; Park, J.S. Heat Transfer Coefficient and Film Cooling Effectiveness on the Partial Cavity Tip of a Gas Turbine Blade. *J. Turbomach.* **2019**, *141*, 071007. [CrossRef]
13. Zhang, Q.; O'Dowd, D.O.; He, L.; Wheeler, A.P.S.; Ligrani, P.M.; Cheong, B.C.Y. Overtip Shock Wave Structure and Its Impact on Turbine Blade Tip Heat Transfer. *J. Turbomach.* **2011**, *133*, 041001. [CrossRef]

14. Zeng, F.; Du, J.; Huang, L.; Xuan, L.; Zhao, Q.; Zou, Z. An Experimental Method for Squealer Tip Flow Field Considering Relative Casing Motion. *Chin. J. Aeronaut.* **2020**, *33*, 1942–1952. [CrossRef]
15. Rhee, D.-H.; Cho, H.H. Local Heat/Mass Transfer Characteristics on a Rotating Blade With Flat Tip in a Low-Speed Annular Cascade—Part II: Tip and Shroud. *J. Turbomach.* **2006**, *128*, 110–119. [CrossRef]
16. Mansouri, Z. Unsteady Simulation of Flow and Heat Transfer in a Transonic Turbine Stage under Non-Uniform Inlet Conditions. *Int. Commun. Heat Mass Transf.* **2021**, *129*, 105660. [CrossRef]
17. Zhang, S.; Ding, S.; Liu, C.; Zhao, G.; Wang, J. A Discussion: Issue Improving the Accuracy of Turbine Blade Heat Transfer Simulation. In *Volume 5B: Heat Transfer—General Interest; Internal Air Systems; Internal Cooling, Proceedings of the ASME Turbo Expo 2021: Turbomachinery Technical Conference and Exposition, Virtual, Online, 7–11 June 2021*; American Society of Mechanical Engineers: New York, NY, USA, 2021; p. V05BT13A003.
18. Timko, L.P. *Energy Efficinet Engine High Pressure Turbine Component Test Performance Report*; NASA Technical Reports, No. NASA CR-168289; National Aeronautics and Space Administration, NASA Lewis Research Center: Cleveland, OH, USA, 1984.
19. O'Dowd, D.O.; Zhang, Q.; He, L.; Ligrani, P.M.; Friedrichs, S. Comparison of Heat Transfer Measurement Techniques on a Transonic Turbine Blade Tip. *J. Turbomach.* **2011**, *133*, 021028. [CrossRef]
20. Xue, S.; Roy, A.; Ng, W.F.; Ekkad, S.V. A Novel Transient Technique to Determine Recovery Temperature, Heat Transfer Coefficient, and Film Cooling Effectiveness Simultaneously in a Transonic Turbine Cascade. *J. Therm. Sci. Eng. Appl.* **2015**, *7*, 011016. [CrossRef]
21. Arisi, A.N. Heat Transfer and Flow Characteristics on the Rotor Tip and Endwall Platform Regions in a Transonic Turbine Cascade. Ph.D. Thesis, Virginia Polytechnic Institute and State University, Blacksburg, VA, USA, 4 December 2015.
22. Kline, S.J. The Purposes of Uncertainty Analysis. *J. Fluids Eng.* **1985**, *107*, 153–160. [CrossRef]
23. Moffat, R.J. Describing the Uncertainties in Experimental Results. *Exp. Therm. Fluid Sci.* **1988**, *1*, 3–17. [CrossRef]
24. Zhong, F.; Zhou, C. Tip Gap Size Effects on Thermal Performance of Cavity-Winglet Tips in Transonic Turbine Cascade with Endwall Motion. *J. Glob. Power Propuls. Soc.* **2017**, *1*, CR5JBC. [CrossRef]